

Fluid-Dynamic and Electromagnetic Characterization of 3D Carbon Dielectrophoresis with Finite Element Analysis

¹Rodrigo Martinez-Duarte, ²Salvatore Cito, ³Esther Collado-Arredondo, ³Sergio O. Martinez and ⁴Marc J. Madou

^{1,4}Mechanical & Aerospace Engineering Department, University of California, Irvine, 4200 Engineering Gateway, Irvine, CA, 92697, USA, tel.: +1 (949) 824-4143

²Universitat Rovira i Virgili, Tarragona, Spain

³Departamento de Ingeniería Eléctrica y Computación, Tecnológico de Monterrey, Campus Monterrey, Monterrey, Mexico

E-mail: ¹drmartnz@gmail.com, ⁴mmadou@uci.edu, ²salvatore.cito@gmail.com, ³smart@itesm.mx

Received: 31 October 2008 / Accepted: 7 November 2008 / Published: 8 December 2008

Abstract: The following work presents the fluid-dynamic and electromagnetic characterization of an array of 3D electrodes to be used in high throughput and high efficiency Carbon Dielectrophoresis (CarbonDEP) applications such as filters, continuous particle enrichment and positioning of particle populations for analysis. CarbonDEP refers to the induction of Dielectrophoresis (DEP) by carbon surfaces. The final goal is, through an initial stage of modeling and analysis, to reduce idea-to-prototype time and cost of CarbonDEP devices to be applied in the health care field. Finite Element Analysis (FEA) is successfully conducted to model flow velocity and electric fields established by polarized high aspect ratio carbon cylinders, and its planar carbon connecting leads, immersed in a water-based medium. Results demonstrate correlation between a decreasing flow velocity gradient and an increasing electric field gradient toward electrodes' surfaces which is optimal for selected CarbonDEP applications. Simulation results are experimentally validated in the proposed applications. Copyright © 2008 IFSA.

Keywords: Carbon, Dielectrophoresis, C-mems, High flow rate, Simulation

1. Introduction

Even when the field of bioparticle separation has advanced significantly in recent years with the wide use of techniques such as Fluorescence-Activated Cell Sorting (FACS) or MACS (Magnetically-

Actuated Cell Sorting) such techniques require the use of specific, and often expensive, tags to achieve high selectivity. An ideal solution would be a technology which eliminates the need of such tags while maintaining a high throughput separation process. We believe Dielectrophoresis (DEP) could be such solution.

Dielectrophoresis refers to the induction of a force, F_{DEP} , on a polar particle immersed in a polar media by a non uniform AC or DC electric field. A huge advantage of DEP over current techniques is its capability to selective manipulate targeted particle(s), by inducing either an attractant or repellent F_{DEP} force to or from the nearest electrode surface, or no force at all, using only the particle's intrinsic dielectric properties (which are solely determined by its individual phenotype such as its surface topography, or membrane morphology, and internal compartmentalization). Such advantage potentially lowers the cost of each assay by eliminating the need of specific tags linked to magnetic beads or fluorophores to discriminate targeted particle types.

Thanks to its intrinsic and unique dielectric properties, each kind of particle presents a particular dielectrophoretic spectrum, F_{DEP} vs. Applied Electric Field's frequency. Fig. 1 is a good example of a conceptual DEP spectrum where F_{DEP} travels from positive to negative as applied frequency changes. When F_{DEP} is positive, it will push the targeted particle(s) towards a higher magnitude electric field area in an electric field gradient, while when being negative it will pull targeted particle(s) from higher magnitude electric field areas to those presenting the minimal magnitude. At the crossover frequency, not necessarily just one, particle will experience zero force. Based on this behavior, a frequency scheme is designed where desired particles are discriminated from the rest of the sample, either by selectively attracting or repelling them from electric field gradient areas, at particular frequency values.

Even when several successful dielectrophoresis applications [review in 1] have been demonstrated with nanometer-thick metallic planar electrodes, as it has been the typical trend until recently, they have generally lacked the ability to achieve throughputs that would justify the wide use of DEP in a clinical setup. The main reason behind this problem is the fact that given a channel cross-section, many targeted particles might flow over the planar electrodes without experiencing any force (see Fig. 2a), its mean distance to the electrode surface being too long, making it necessary to employ "tricks" such as re-flowing the same sample several times to obtain a high throughput.

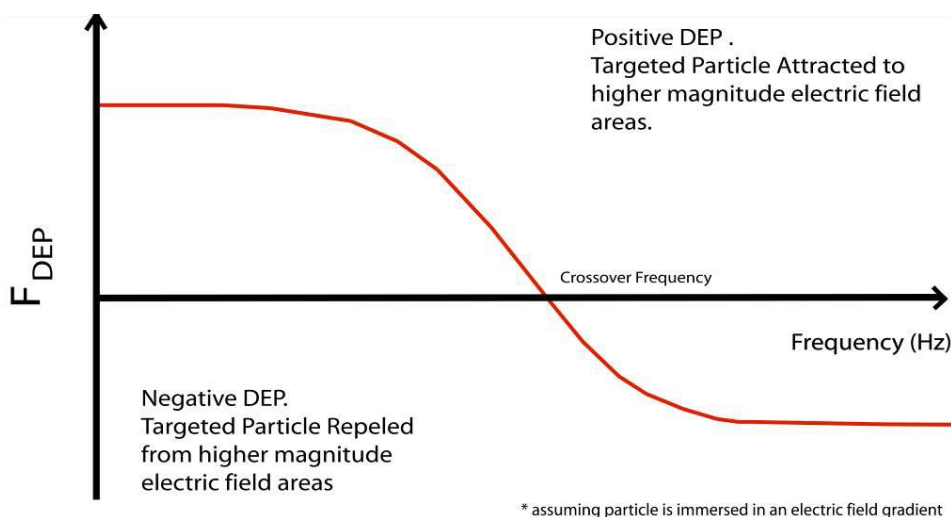


Fig. 1. A conceptual DEP spectrum. When F_{DEP} is positive, it will push the targeted particle(s) towards a higher magnitude electric field area in an electric field gradient, while when being negative it will pull targeted particle(s) from higher magnitude electric field areas to those presenting the minimal magnitude. At the crossover frequency, not necessarily just one, particle will experience zero force.

The use of volumetric (3D) structures allows higher throughput than traditional planar DEP devices [2] in the quest for values comparable to current separation techniques ($>50,000$ cells per second). The difference in trapping efficiency, when only flowing the sample once, between 2D and 3D electrodes drastically increases as flow rate increases being 2D efficiency always the less when compared to 3D's. The main concept behind using 3D structures is to reduce the mean distance of any targeted particle contained in a channel or chamber to the closest electrode surface (Fig. 2b).

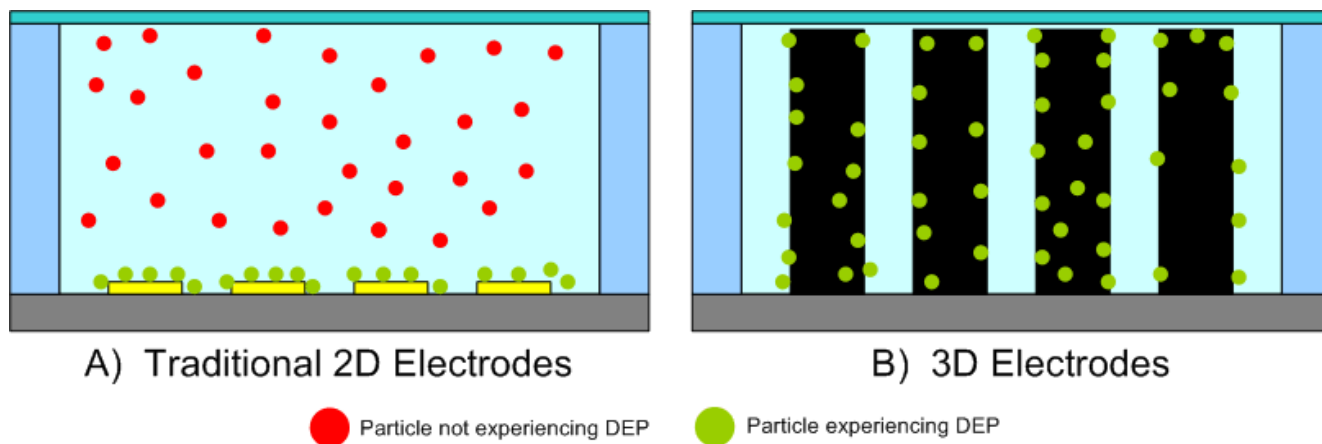


Fig. 2. Comparison between 2D and 3D electrodes. Given a channel cross-section, many targeted particles might flow over the planar electrodes without experiencing any force (A), its mean distance to the electrode surface being too long, making it necessary to employ “tricks” such as re-flowing the same sample several times to obtain a high throughput. The main concept behind using 3D structures (B) is to reduce the mean distance of any targeted particle contained in the channel to the closest electrode surface thus allowing to achieve high throughput in a flow-once scheme. The advantage of using 3D structures becomes more significant as one increases the height of the channel ($> 40 \mu\text{m}$).

Microfabricated volumetric electrodes have been implemented by Wang [3] and Voldman [4] who used electroplated gold electrodes for particle separation applying the lateral field established by the electrodes on channel side-walls and for particle trapping for cytometry purposes respectively. More recently, Iliescu [5] has used complex microfabrication techniques to obtain volumetric doped silicon electrodes in a multi-step process. In a non-traditional way, Lapizco-Encinas, Cummings, Fintschenko et al [6] have induced DEP on bacteria and proteins using insulator volumetric microelectrodes which has become to be known as insulator DEP. The main concept behind this approach is the use of two metal electrodes, excited by thousands of volts at DC, to generate a uniform electric field between them which is then disrupted, and turned non-uniform, by the insulator structures. Other true 3D approach, although not technically microfabricated, is that of Fatoyinbo, Hughes et al [7], who in an elegant solution, used a drilled insulator-conductor sandwich to obtain wells with electrodes all along their walls.

We propose the use of 3D Carbon Dielectrophoresis (CarbonDEP). CarbonDEP refers to the use of carbon surfaces to induce DEP. In our case, such surfaces penetrate the bulk of the sample (3D). Carbon surfaces offer 1) better electrochemical and biocompatibility properties than other conductive materials [8], 2) chemical inertness to mostly all solvents, 3) excellent mechanical properties, and 5) although its conductivity does not compare to metals, is still quite good for dielectrophoresis applications [9].

Even when carbon surfaces might be fabricated by several different ways, we have employed the Carbon MEMS (C-MEMS) technique [8]. C-MEMS refers to a fabrication technique where carbon is

obtained through the pyrolysis of certain polymers such as photoresists. Precursor polymer might be patterned by photolithography [8, 10], lithography, stamping [11], molding, embossing or any other suitable technique. Important is to note that different degrees of isometric shrinkage, depending on structure size and precursor chemical composition, are obtained during pyrolysis [9]. The use of the C-MEMS technique affords a simple, rapid and relatively inexpensive fabrication process that allows a) High Aspect Ratio (HAR) structures, b) precise control of device dimensions and complexity, c) high quality precursors and d) excellent repeatability.

In the following work we present initial models and analysis of a proposed 3D CarbonDEP array to characterize its advantages. The use of Finite Element Analysis is towards implementing a design and fabrication methodology leading to shorter development times of CarbonDEP applications in the health care field. In contrast to previous work where 3D electrodes arrays made out of a perfect conductor and immersed in DI water [12] or only simplified planar geometries in conductive media are simulated [9], we have modeled and analyzed both electric and flow velocity fields independently in an array of polarized carbon 3D electrodes and their 2D connection leads immersed in a water-based medium. Simulated geometry is a close approximation to the experimental device. Experimental validation and examples of applications are also detailed.

2. Materials and Methods

2.1. Experimental

Our 3D CarbonDEP device is a flow-through microfluidic channel with embedded carbon posts. Device integrates three main blocks: 1) carbon posts, 2) microfluidic network and 3) external interfacing.

In order to fabricate carbon posts we followed the C-MEMS technique using SU-8 (MicroChem, US) as precursor resist. The substrate material was silicon with a 500 nm layer of silicon dioxide grown thermally to act as an electrical insulator. The complete process is shown in Fig. 3 for a 5×29 array of posts (3D). SU-8 posts (130 μm high and 50 μm diameter) and leads were fabricated in a two-step photolithography sequence (Fig. 3a) and were then carbonized by pyrolysis at 900 °C in a Nitrogen/Forming Gas environment. Fig. 3b shows the resulting carbon electrodes and connecting leads. CarbonDEP array features 60 μm high post electrodes with a 25 μm diameter. The gap between electrodes in the axis parallel to the channel wall is 40 μm while it is 100 μm in the perpendicular one. In order to prevent leads from being physical obstacles and to protect them from lifting off, the channel bottom was planarized by a 1.4 μm layer of SU-8 (Fig. 3c). A 500 μm wide, 65 μm high channel was then fabricated using SU-8 (Fig. 3d). Channel was closed, by placing a glass lid using SU-8 as adhesive, in such a way that it features SU-8 on the four walls. As the final step, device was sealed with transparent epoxy.

External interfacing comprised electrical connections made by coating carbon pads with silver conductive paint and subsequently soldering an AWG18 wire lead to the silver coat. Nanoport assemblies and PEEK tubing (Upchurch Scientific, USA) were used to interface dispensing apparatus and waste reservoirs to channel's inlet and outlet respectively.

The geometry employed for simulations is based on the experimental device. Given the symmetry of the CarbonDEP array, its length was reduced from 5 X 29 to 5 X 5 to reduce computational power requirements.

2.2. Electromagnetic Analysis

Electromagnetic simulation was conducted using COMSOL v3.3 (COMSOL) running in a Workstation having Solaris 9 (Sun Microsystems) as operating system (OS). Processor used was a Sun Blade 1500 @ 1 GHz. 2 GB of RAM and up to 5 GB of Virtual Memory were at hand.

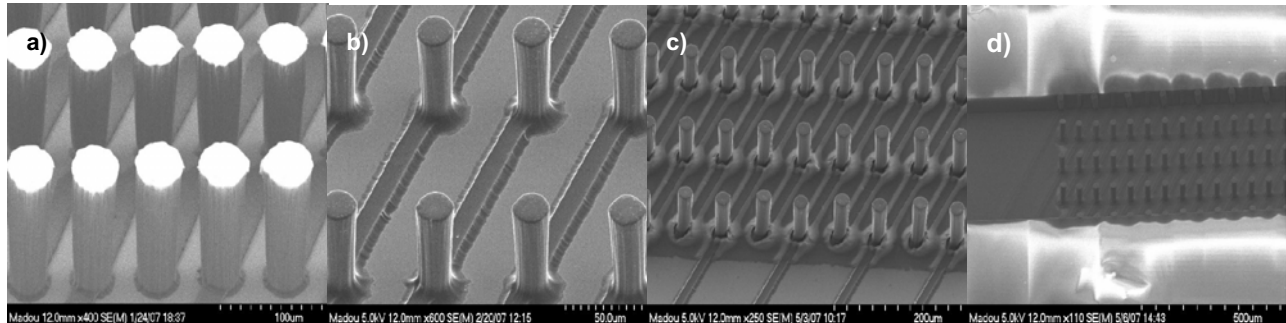


Fig. 3. Experimental device fabrication sequence. (a) Two-step photolithography of SU-8 to obtain connecting leads and 130 μm high, 50 μm diameter SU-8 posts. (b) After pyrolysis at 900 $^{\circ}\text{C}$ in a Nitrogen/Forcing gas atmosphere (following the C-MEMS technique), SU-8 posts and leads transform into carbon electrodes (60 μm high, 25 μm diameter). (c) A 1.4 μm high SU-8 layer is patterned around carbon electrodes to planarize channel bottom and prevent carbon leads from lifting off while immersed in an aqueous media. (d) A 500 μm wide, 65 μm high channel is patterned around electrode array by SU-8 photolithography. Pictures taken with a Hitachi S-4700-2 FESEM Scanning Electron Microscope.

Analysis is completed by separately meshing connecting leads and carbon posts using Triangular 2D meshes and implementing coupling through identity boundary conditions. Carbon structures were considered to have an equal resistivity at all points of $1.07 \times 10^{-4} \text{ W}\cdot\text{m}$ [9]. Electrodes are assumed to be in contact with a water medium of conductivity equal to 2 mS/m . Excitation voltage was 4 V_{pp} . Boundary conditions are those of an insulator in all channel walls and in channel regions furthest away from electrode array.

2.3. Fluidodynamic Analysis

Computational Fluid Dynamics (CFD) simulation was conducted using Fluent 6.3.26 (ANSYS, Inc.). Analysis was done numerically by solving the Navier-Stokes equation in a 3D structured grid using an absolute velocity formulation with a relaxation factor of 0.3 for the pressure, density body forces and momentum variables. Problem has been solved in steady condition as a fully developed flow assuming a Newtonian flow with water as a fluid. Boundary conditions are those of No-slip imposed on the channel walls and carbon posts' surface. A 3D pressure-based laminar approach has been considered with a mass-flow channel inlet of $1.6 \times 10^{-7} \text{ kg}/\text{s}$ and an outflow boundary condition at the outlet. Such condition assumes a zero normal gradient for all flow variables except pressure. Velocity and pressure have been coupled using the standard SIMPLE model that uses a relationship between velocity and pressure corrections to enforce mass conservation and to obtain the pressure field. For the numerical discretization of pressure and Momentum, a second order upwind scheme has been used.

3. Results

3.1 3.1. Electromagnetic

Isometric views of the induced electric field distribution at 10 μm from the channel floor (Fig. 4a) and at 60 μm (Fig. 4b) are shown together. Important is to note that electromagnetic simulation does not take the thin SU-8 layer on channel floor into account. As a result, carbon leads are simulated in direct contact with media. As expected, at 10 μm from channel floor one can discern a fairly strong electric field gradient induced by the connection leads (Fig. 4a). It is expected that such field would get greatly attenuated if one factors in the effect of an insulating layer (SU-8) on top of the connecting leads as in the experimental device. At 60 μm , near the top of the channel, the electric field gradient induced by the leads completely vanishes and the one generated by the carbon posts predominates. A detailed top view of the 30 μm cross section of the array (Fig. 5a) shows how even at 30 μm from the channel bottom leads do not have a role in the induced electric field. Fig. 5b is a X-Z cross section at slice # on Fig. 5a clearly showing how the effect of the leads diminishes as distance from the channel floor increases and disappears at around 20 μm .

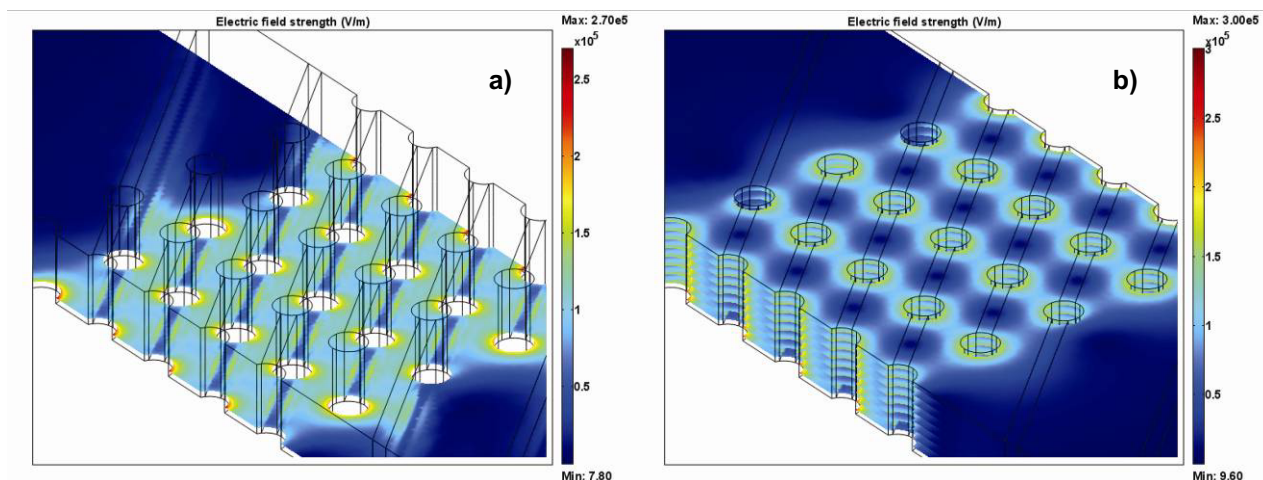


Fig 4. Induced electric field distribution by a polarized carbon electrode array at $4 V_{pp}$ immersed in a 2 mS/m conductive media. 1.4 μm high SU-8 layer planarizing channel bottom present in experimental device is not simulated. Leads are assumed to be in direct contact with media. (a) Isometric view at 10 μm from channel bottom. A fairly strong electric field is induced by the connection leads at the channel bottom. (b) Isometric view at 60 μm from channel bottom showing how the electric field induced by posts predominates. Lighter blue denotes those areas with an electric field magnitude of $\sim 1 \times 10^5$ V/m. Yellow denotes magnitudes of $\sim 2 \times 10^5$ V/m while darker blue denotes those areas with a magnitude near zero. Positive DEP will be induced on those particles contained in areas of higher magnitude (light blue, yellow, red) while Negative DEP will be induced in darker blue areas.

3.2. Fluido-dynamic

3D Flow velocity field is shown in Fig. 6a. X-Y, X-Z and Y-Z cross sections are shown in Fig. 6b, c and d respectively. In this case, the thin layer of SU-8 covering electric leads on channel bottom is taken into account. A planar channel floor is thus assumed. Channel walls and electrode surfaces were assumed to be flat to simplify analysis even when experimental device does show minimal roughness on the mentioned surfaces. Results clearly show a parabolic flow profile in between electrodes as corroborated by Fig. 7a in the case of the X-Y plane. Furthermore, a velocity magnitude decreasing gradient towards electrode surfaces is induced by the proposed geometry. Circular posts geometry is also shown to minimally disturb pathlines established by laminar flow in our device.

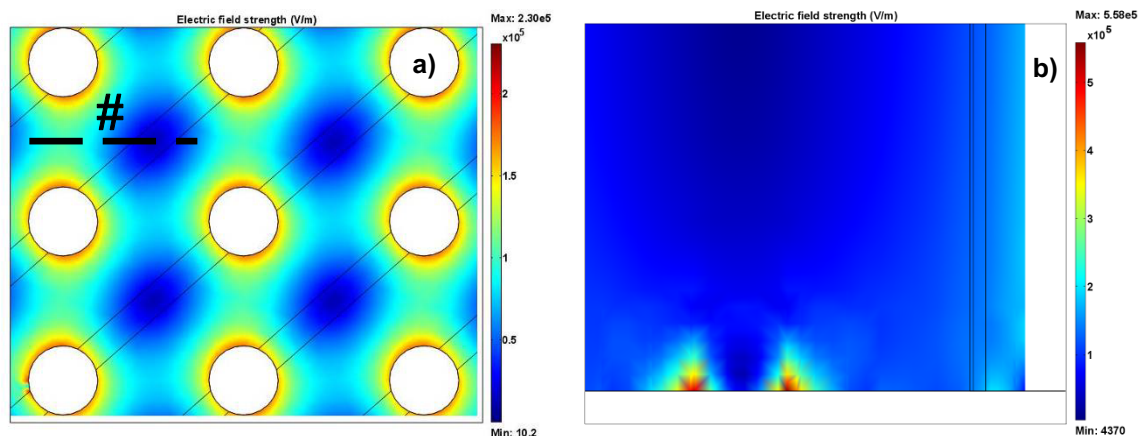


Fig. 5. (a) Detailed top view (X-Y) at 30 μm from the channel floor showing how the effects of leads tend to disappear even at this height. Also note how an increasing electric field gradient is established towards electrodes surfaces (white circles) and how the minimal magnitude of electric field is present on those points furthest away from electrodes. Color scale is the same as in Fig 4. (b) X – Z cross section at slice # in 5A. Note how the electric field gradient induced by connection leads in channel bottom quickly vanishes at around 20 μm from channel floor. Lighter blue regions denote those areas with an electric field magnitude of $\sim 2 \times 10^5$ V/m. Yellow regions denote magnitudes of $\sim 3.5 \times 10^5$ V/m while darker blue areas denote those areas with a magnitude near zero. Positive DEP will be induced on those particles contained in areas of higher magnitude (light blue, yellow, red) while Negative DEP will be induced in darker blue areas.

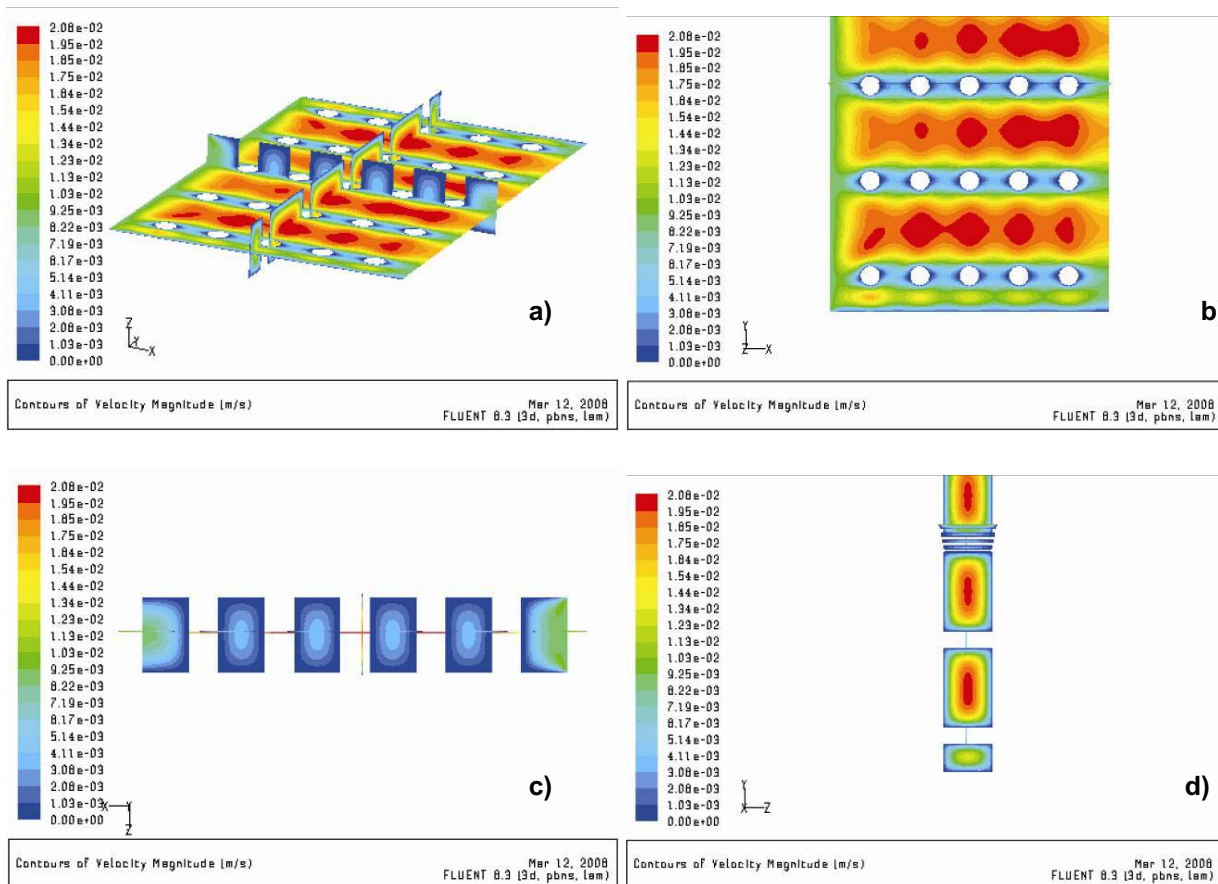


Fig. 6. Simulation results showing the flow velocity field in a carbon electrode array for a 10 $\mu\text{l}/\text{min}$ flow: (a) 3D model, (b) X – Y, (c), X – Z and (d) Y – Z cross sections. Note the established 3D parabolic flow profile. Darker blue areas denote areas of zero flow velocity, green areas those of $\sim 1 \times 10^{-2}$ m/s and red areas those of highest magnitude ($\sim 2 \times 10^{-2}$ m/s). Note how a decreasing flow velocity gradient is established towards electrodes' surfaces (white circles) and channel walls due to the no-slip condition existent on such surfaces.

4. Experimental Validation and Applications

Experimental platform featured four main components: 1) DEP device and its external interfacing, 2) a Stanford Research Systems AC Signal Generator Model DS345, 3) a Motic Microscope, Model PSM1000, interfaced to a Costar Imaging SI-C400N CCD camera or a Nikon Eclipse LV100D Microscope interfaced to SPOT#7.4 Slider CCD camera and a 4) Harvard Apparatus PHD2000 Infuse/Withdraw Pump as a dispensing apparatus.

Experimental samples included 1) 8 μm latex particles (Duke Scientific Corporation, US) suspended in DI water, 2) viable yeast grown overnight in Sabouraud medium (30 g/l) at 30° C and 250 RPM, washed and re-suspended in water with peptone (6 g/l) to give a conductivity of 51 mS/m (this sample featured a $\sim 20\%$ non viable yeast), and 3) non viable yeast, rendered non viable by a 0.5 hour water bath at 90°C, suspended in DI water.

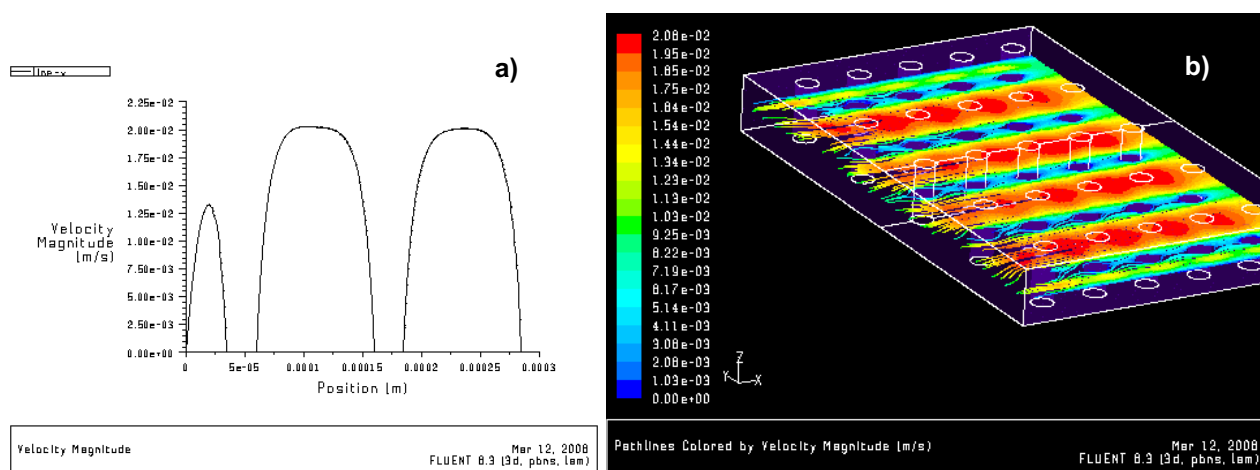


Fig. 7. (a) Parabolic profile established in between electrodes in the X-Y plane. Note the maximum velocity of 2.09×10^{-2} m/s and how the gap between electrodes allows for a plug-like flow profile on those areas further away from electrode surfaces. (b) Pathlines of a laminar flow in our carbon array. Note the continuity of the pathlines going through the carbon post array and how they follow the contours of posts surfaces.

Fig. 8 compares experimental and simulation results. A successful correlation between the Negative and Positive DEP areas obtained experimentally with those predicted by FEA has been achieved. Latex particles in a stationary flow are clustered by Negative DEP in the lowest electric field magnitude areas when electrode array is polarized by a sinusoidal signal at 5 MHz and 10 V_{pp} . Non viable yeast are extracted from a 10 $\mu\text{l}/\text{min}$ flow and trapped by Positive DEP in the highest electric field magnitude areas. In this case electrode array was polarized by a sinusoidal signal at 100 kHz and 10 V_{pp} .

4.1. Filter

Fig. 9a shows the filtering of viable yeast from non viable yeast when establishing a 10 $\mu\text{l}/\text{min}$ flow (from left to right). Viable yeast are being trapped by Positive DEP in those areas predicted by electromagnetic simulation. Experimental details and filter efficiencies for different flow rates are described elsewhere [2]. The correlation of a decreasing flow velocity gradient and an increasing electric field gradient towards electrode surface improves trapping by Positive DEP in this case. Fig. 9b shows a 2-stage filter. Two independent electrode arrays are independently excited by different

optimized sinusoidal signals on their magnitude and frequency to selectively trap targeted particle(s) in different arrays. In this case, viable yeast are being trapped on the left array while non viable yeast are trapped in the right array. Fabrication and experimental details can be found elsewhere [13].

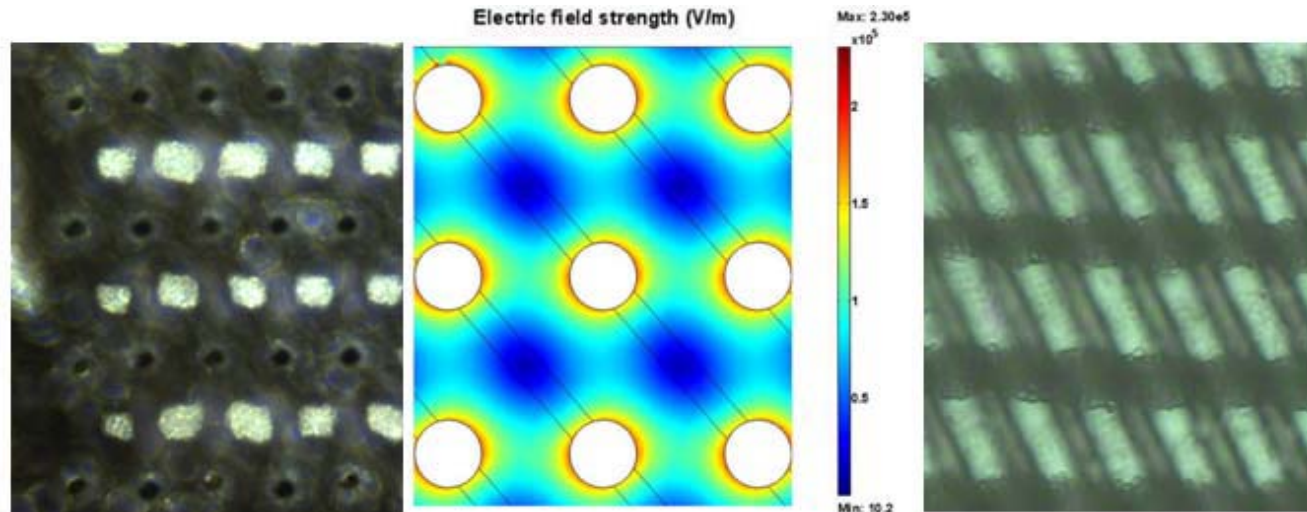


Fig. 8. Comparison between experimental (left and right images) and simulation (middle image) results showing a successful correlation. Darkest blue areas in the simulation results denote regions of lowest electric field magnitude and NegativeDEP while lighter blue, yellow and red denote the increasing electric field magnitude gradient towards electrode surface (white circles) and PositiveDEP. Latex beads on left image (carbon posts can be identified as the dark smaller circles, latex beads appear in white) are clustered into Negative DEP areas (compare to darkest blue in middle image) while non viable yeast (right image) are extracted from a 10 $\mu\text{l}/\text{min}$ and trapped on Positive DEP areas (compare to lighter blue areas). Both latex and non viable yeast are suspended in DI water. Left and right pictures were taken with a CCD camera interfaced to a microscope while focusing the top of the electrodes ($\sim 60 \mu\text{m}$ from channel bottom).

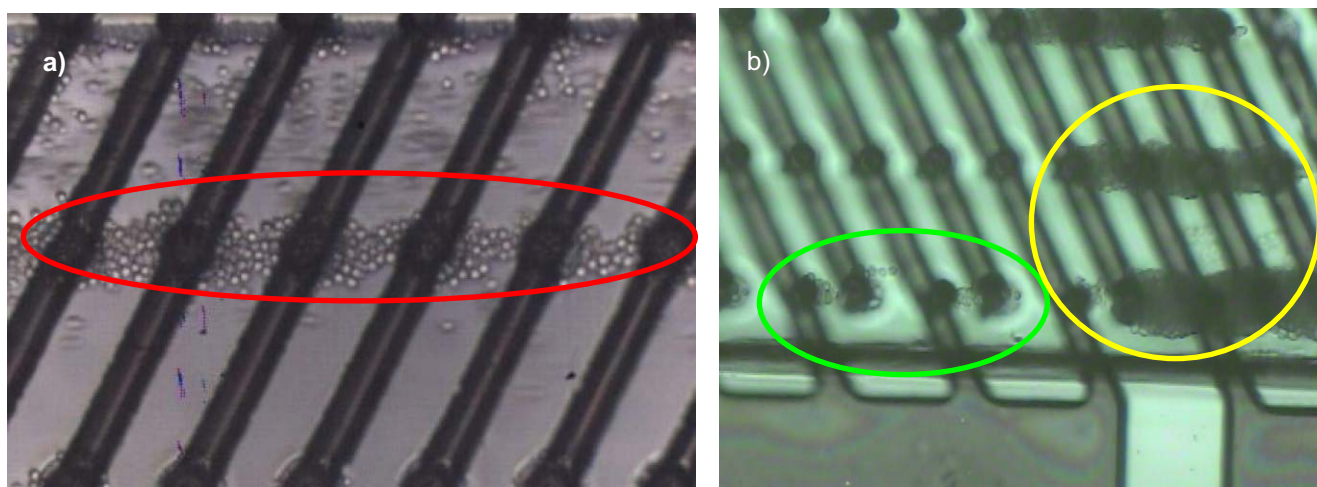


Fig. 9. (a) Viable yeast (in red ellipse) being filtered from Non viable yeast (blurred moving particles) against a 10 $\mu\text{l}/\text{min}$ flow using a polarized CarbonDEP array by a sinusoidal signal at 5 MHz and 10 V_{pp} . Medium conductivity is 51 mS/m . Viable yeast are being trapped by PositiveDEP in those areas predicted by electromagnetic simulation. (b) A two-stage filter featuring two independent CarbonDEP arrays each of them excited by optimized sinusoidal signals to trap viable (green circle, left side) and non viable (yellow circle, right side) yeast.

4.2. Continuous Enrichment

Fig. 10 shows the continuous enrichment of viable yeast by Positive Dielectrophoresis Focusing. The principle works when the hydrodynamic force overcomes the PositiveDEP trapping force. Since laminar flow is established in the channel and pathlines have been shown to be minimally disturbed by our array geometry, viable yeast flushes away contained in those pathlines co-linear with the polarized electrode rows (and PositiveDEP areas). Such principle allows continuous separation at higher flow rates than those achieved when implementing separation by trapping, such as in a filter, but requires more complicated geometries for enriched population retrieval.

5. Discussion

Applications of advantages achieved when using 3D CarbonDEP have already been detailed. Of most importance is the fact that the electric field gradient increases while flow velocity field gradient decreases as one moves towards the electrode surfaces'. Such correlation proves to be optimal for PositiveDEP trapping since F_{DEP} is at its maximum where velocity magnitude is at its minimum requiring then less force, and thus less polarizing voltage, to maintain targeted particle(s) at desired locations. On the other hand, particle(s) selectively pulled into NegativeDEP areas can be quickly eluted and collected at the channel's end in a continuous basis.

Thanks to the different spacing between electrodes in the X and Y axis (spacing is shorter in the X axis) it is possible to restrict the trapping of desired particles by PositiveDEP, and the subsequent particle cluster, to areas that would minimally disturb the pathlines and maintain the laminar flow.

Note the space correlation between simulation and experiments, in Fig. 8, even when electrode array is polarized by a 4 V_{pp} signal on simulation and a 10 V_{pp} one in experiments. Such correlation suggests a significant voltage drop on carbon structures from connection pad to the active DEP area. Voltage drop was expected given the fact that our carbon has a conductivity which is about three orders of magnitude less than that of metals. Future work will be aimed on quantifying such voltage drop.

Even when a successful correlation between experimental and simulation results was achieved, it is important to consider a few improvements on the modeling and characterizing methodology such as the inclusion of the SU-8 thin layer in future electromagnetic simulations. A full characterization on the electric field induced by different geometries immersed in different medium conductivities and polarized by different signal parameters will also be conducted. Results will allow us to optimize parameters towards reducing the time of converting an idea into a working prototype for future CarbonDEP devices.

6. Conclusions

An initial methodology to model and characterize CarbonDEP devices has been successfully correlated with experimental results. We have demonstrated how our 3D CarbonDEP array 1) achieves higher throughput by inducing positive and negative DEP regions in the bulk of the channel and not only in the vicinity of channel walls as in the case of traditional 2D DEP systems, 2) induces an increasing electric field magnitude gradient towards the electrodes' surfaces, 3) establishes a decreasing flow velocity gradient towards the electrodes' surfaces, 4) establishes an optimal correlation between a decreasing flow velocity gradient and increasing electric field gradient toward electrodes' surfaces and 5) do not create physical traps by minimally disturbing the flow path lines. Application of such facts has been detailed towards engineering high throughput DEP devices capable of offering a lower-cost alternative to current separation techniques.

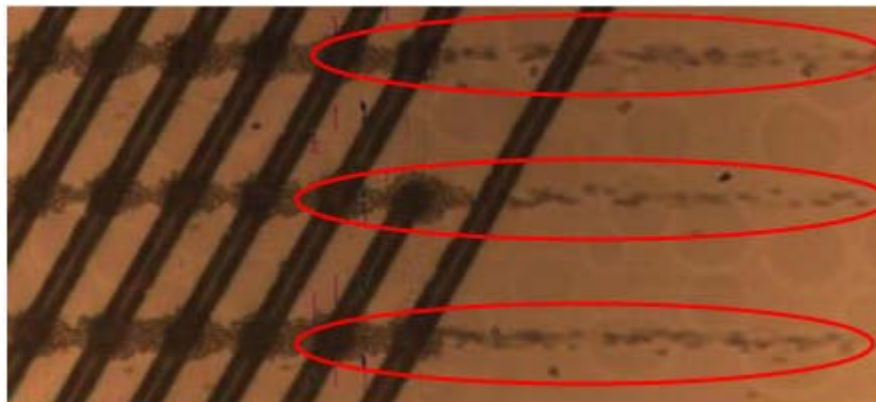


Fig. 10. Continuous enrichment of viable yeast (red ellipses) at 20 $\mu\text{l}/\text{min}$ with a polarized CarbonDEP array at 1 MHz and 10 V_{pp} . Medium conductivity is 51 mS/m. The principle works when the hydrodynamic force overcomes the PositiveDEP trapping force. Such principle allows continuous separation at higher flow rates than those achieved when implementing separation by trapping, such as in a filter, but requires more complicated geometries for enriched population retrieval. The goal of this scheme is to only attract targeted particles to certain areas where they can be flowed out in characteristic lines such as the ones shown.

Acknowledgements

This work was supported in part by the University of California Institute for Mexico and the United States (UC MEXUS), award number UCM- 40117 through the University of California, Irvine – Tecnológico de Monterrey Alliance for Micro/Nanotechnology based Entrepreneurship. Thanks to members of the Madou BIOMEMS research group and INRF at UCI for valuable discussions and support.

References

- [1]. P. Gascoyne, J. Vykoukal, Dielectrophoresis-Based Sample Handling in General-Purpose Programmable Diagnostic Instruments, in *Proceedings of the IEEE*, 92, 1, 2004, p. 22.
- [2]. R. Martinez-Duarte, H. A. Rouabah, N. G. Green, M. Madou and H. Morgan, Higher Efficiency and Throughput in Particle Separation with 3D Dielectrophoresis with C-MEMS, in *Proceedings of the 11th International Conference in Miniaturized Systems for Health and Life Systems: microTAS 2007*, Paris, France, 7-11 October 2007, p. 828.
- [3]. L. Wang, L. Flanagan, A. P. Lee, Side-Wall Vertical Electrodes for Lateral Field Microfluidic Applications, *Journal of Microelectromechanical Systems*, 16, 2, 2007, p. 454.
- [4]. J. Voldman, M. Gray, M. Toner, M. Schmidt, A Microfabrication-based Dynamic Array Cytometer, *Analytical Chemistry*, 74, 2002, p. 3984.
- [5]. C. Iliescu, L. Yu, G. Xu, F.E. H. Tay, A Dielectrophoretic Chip With a 3-D Electric Field Gradient, *Journal of Microelectromechanical Systems*, 15, 6, 2006, p. 1506.
- [6]. B. H. Lapizco Encinas, B. A. Simmons, E. B. Cummings, Y. Fintschenko, Dielectrophoretic Concentration and Separation of Live and Dead Bacteria in an Array of Insulators, *Analytical Chemistry*, 76, 6, 2004, p. 1571.
- [7]. H. Fatoyinbo, D. Kamchis, R. Whittingham, S. L. Ogini, M. Hughes, A High-Throughput 3-D Composite Dielectrophoretic Separator, *IEEE Trans on Biomedical Eng.* 52, 7, 2005, p. 1347.
- [8]. C. Wang, G. Jia, L. Taherabadi, M. Madou, A Novel Method for the Fabrication of High Aspect Ratio C-MEMS Structures, *IEEE Journal of MEMS*, 14, 2, 2005, p. 348.
- [9]. B. Y. Park, L. Taherabadi, C. Wang, J. Zoval, M. J. Madou, Electrical Properties and Shrinkage of Carbonized Photoresist Films and the implications for Carbon Microelectromechanical Systems Devices in Conductive Media, *Journal of Electrochemical Society*, 152, 12, 2005, p. J136.

- [10].B. Y. Park, R. Zaouk, M. J. Madou, Validation of lithography based on the controlled movement of light-emitting particles, SPIE Microlithography, *Emerging Lithographic Technologies VIII*, SPIE, Bellingham, WA, 2004, p. 566.
- [11].A. L. Das, R. Mukherjee, V. Katiyer, M. Kulkarni, A. Ghatak, A. Sharma, Generation of Sub-micrometer-scale Patterns by Successive Miniaturization Using Hydrogels, *Advanced Materials*, 19, 2007, p. 1943.
- [12].B. Y. Park, M. J. Madou, 3-D electrode designs for flow-through dielectrophoretic systems, *Electrophoresis*, 26, 2005, p. 3745.
- [13].R. Martinez-Duarte, J. Andrade-Roman, S. O. Martinez and M. Madou, A High Throughput Multi-stage, Multi-frequency filter and separation device based on Carbon Dielectrophoresis, in *Proceedings of the NSTI-Nanotech 2008*, Boston, MA, 1-5 June 2008, 3, 2008, p. 316.

2008 Copyright ©, International Frequency Sensor Association (IFSA). All rights reserved.
(<http://www.sensorsportal.com>)

ISSN 1726-5479

Advertise in *Sensors & Transducers Journal*



http://www.sensorsportal.com/DOWNLOADS/Media_Kit_2008.pdf
sales@sensorsportal.com